LAWRENCE
LIVERMORE
NATIONAL
LABORATORY

UCRL-JRNL-224594

Fluctuations and Gibbs-Thomson Law - the Simple Physics.

A. A. Chernov, J. J. De Yoreo, L. N. Rashkovich

September 21, 2006

Journal of Optoelectronic s and Advanced Materials

Updated October 14, 2003

Fluctuations and Gibbs-Thomson Law – the Simple Physics.

A.A.Chernov*, J.J.DeYoreo*, L.N.Rashkovich**
* Lawrence Livermore National Laboratory, 7000 East Avenue, Livermore CA 94550, USA
** Moscow State University, 119992 Vorobyevy Gory, Moscow, Russia

Abstract

Crystals of slightly soluble materials should be subject of relatively weak attachment/detachment fluctuations on their faces so that steps on that faces have low kink density. These steps are parallel to the most close packed lattice rows and form polygons on a crystal surface. The process responsible for implementation of the classical Gibbs-Thomson law (GTL) for the polygonal step (in two dimensions, 2D) is kink exchange between the step corners. For the 3D crystallites, this mechanism includes step exchange. If these mechanisms do not operate because of slow fluctuations the GTL is not applicable. Physics of these processes and conditions for the GTL applicability are discussed on a simple qualitative level.

In our last publications, partly summarized in [1] and presented in more detail at ROCAM 2006 we discussed behavior of steps with low kink density. Such steps demonstrate that the premise on intensive step fluctuations traditionally accepted after an example estimate in the classical work of Burton Cabrera and Frank (BCF) [2] may not be valid [3,4,5]. Also, low kink density can make the Gibbs-Thomson law (GTL) not applicable to correct crystallization driving force for the small objects. This textbook law quantifies the capillarity induced increase of equilibrium solution concentration or the vapor pressure above a small crystallite or an island of a new lattice layer. When the GTL correction is violated, predictions of the BCF theory on the spiral growth rate and spiral morphology should be generalized correspondingly.
In this note we reiterate basic physics of why and under what conditions the GTL is or is not applicable.

1. Steps with high and low kink density.

At any temperature $T>0$, atoms, molecules or ions of which a crystal is built may detach from the step, i.e. from the end of the incomplete lattice layer on the crystal surface. Also, at $T>0$, these species are present in solution or vapor in dynamic phase equilibrium with the crystal so that they attach to the step. This exchange results in uncompleted

lattice rows on the step. Each row is terminated by two "kinks" of the opposite sign on the step. Presence of these kinks means that the step is not a straight line: the step meanders over the crystal face. This meandering is the step fluctuation. The intensively fluctuating ("rough") steps are illustrated by Fig. 1[6]. Six steps on the (111) face of the FCC ferritin crystal are visible on this AFM image. Ferritin is a big (M = 450,000 Da) iron storage protein which molecules are spheres ~13nm in diameter seen in the image. Average distance between kinks in Fig. 1 is ~ 4 molecular diameters. Fig 2 demonstrates the opposite case of weak fluctuations of steps on the lysozyme crystal (lysozyme is also a protein, M=14,300 Da). In Fig. 2, the average distance between kinks is ~ 500nm, i.e. ~ 100 lattice spacing. Macroscopically, the steps with low kink density (the "smooth" steps) are straight and are oriented along the most densely packed crystallographic directions in the lattice.

Closed loop of a smooth step takes a polygonal shape. The rough step is rounded so that a closed loop is about circular because in this case the step free energy or the growth rate is nearly isotropic.

A step is smooth or rough depending of how much energy costs its meandering, i.e. the entropy increase because of the kink creation. The measure is the kink energy, ε (in the thermal units kT, i.e. ε/kT). At or close to the phase equilibrium, the number of kinks per unit length along the step (the kink density), is $\sim (2/a)\exp[-\varepsilon/kT]$ [2]. The larger the ε/kT the lower the kink density. The kink energy ε is the energy of the step riser per molecule and is often comparable with a half of the excess intermolecular bond energy directly related to solubility. Therefore approximate empirical relationships between solubility and the surface energy, see e.g. [7, 8], suggest higher kink energy for the salts of lower solubility. One of them [7] presents the surface energy per molecular site in kT units as $\varepsilon/kT \approx -0.272 \ln C_e$ (mol/m^3) + 2.82. The free surface energies used to establish these relationships were obtained from experiments on nucleation of salts in aqueous solutions. Thus these energies are averaged over various crystal faces and may be underestimated because of possible heterogeneous nucleation. Difference between potential and the free energy was also not taken into account. This may cause additional underestimate in the surface/kink energy.

Sparingly soluble salts, including biominerals like Ca or Mg carbonates, e.g. calcite $CaCO_3$, or phosphates have low solubilities and therefore high kink energy. The steps on their faces are indeed typically straight. Semiconductors in contact with vapor at sufficiently low temperatures provide other examples.

Kink density that is at least several times lower the maximum ~$2/a$ means than the step rate must be essentially limited not only by the rate at which a kink propagates along the step but also by the kink generation rate. This statement is directly confirmed by the AFM observation of steps on brushite [1]. Namely, as soon as two straight steps come across one another creating reentrant corner, one of the steps is accelerated until the reentrant corner exists. The reason is that the reentrant corner already has a kink configuration (Fig 3). As long as the corner exists, it serves as a continuous kink source. The source power is proportional to the rate at which single ions attach to that corner and

a new lattice row splits from the corner to propagate along the step. The observed step acceleration suggests that the splitting rate exceeds the rate at which the kinks are generated by one dimensional (1D) nucleation. It is not clear, however, what limits the splitting source power and prevents rounding of the reentrant corner. Another evidence of the limiting role of the kink generation on the step rate is nonlinear dependence of the step rate on calcite on supersaturation [9]

Polygonal shape of the step loops or spirals also suggests that fluctuations are not fast enough to provide kink density approaching its maximum ~ $2/a$. Indeed, all steps parallel to the non close packed lattice orientations possessing numerous kinks for geometrical structural reasons move essentially faster than the smooth steps along the close packed directions. As a result, all the kink-rich step orientations wedge out.

2. Gibbs-Thomson law in liquids vs crystals.

Fig.4 is a visual aid to think on how the GTL is implemented in a liquid and in a crystal. Imagine a small liquid droplet or a crystallite immersed in its vapor or solution. We assume this gaseous or liquid solution to be saturated with respect to the bulk (infinite) liquid or crystal. The chemical potential of the species under consideration in either of these solutions is μ_∞. Let us assume that the droplet or the crystallite size L is small, ~10-100 times larger capillarity length $\omega\alpha/kT$ (typically, ~1nm). Here ω and α are specific molecular volume and free surface energy, respectively. Then, according to the GTL, both the droplet and the crystallite must dissolve (evaporate) since the chemical potential of the species in it is larger by $\omega\alpha/L$ than in the surrounding medium (cf. Fig.4). However, the dissolution process must be different in the droplet and the crystallite for the following reasons.

When a particle leaves the droplet the hole in the liquid is filled quickly via molecular rearrangement. In macroscopic terms, the same leveling of a dip on the droplet surface and the corresponding shrink of the droplet diameter L occurs at the speed of sound (~km/s) equilibrating difference in the capillarity pressure under different portion of the perturbed liquid surface. Local variation in the droplet shape is also corrected (though slower) by capillarity waves (at the rate $>\sim (2\pi\alpha/\rho L)^{1/2} \sim 20$m/s for L=1μm, α=80dyn/cm^2). In simple words, any the information on detachment (and attachment) of species spreads over the droplet about immediately. In other words, each molecule or ion "knows" the droplet size at any moment of time. Consequently, chemical potential (detachment work) of each particle depends on the droplet size L at that time.

In a solid, there is no capillarity pressure α/L similar to that in a liquid since there is no easy particle rearrangement (besides surface relaxation and reconstruction). The surface energy in solids is different from the surface tension [10-13]. The latter is described by surface stress tensor, f_{ij}. This tensor comes from such a variation of the Gibbs free

surface energy that is associated only with its mechanical strain (say, by unilateral stretching or compression) while the amount of species in the solid is kept constant. The f_{ij} are the derivatives of surface energy α with respect to the strain (deformation) tensor components. The f_{ij} are different from α and may have not only negative but also positive components [13]. The described elastic variation is fundamentally different from the variation during which the solid surface is being changed due to adding or detaching particles to the solid. This is the latter rather the former (elastic) variation mode that leads to the condition of the phase equilibrium and provides the Gibbs-Thomson term $\omega\alpha/L$ to the equality of chemical potentials between the phases. The surface induced stress in a solid is $\sim f/L$. It adds the energy $\sim \omega(f/L)^2/2G$ to the chemical potential of that solid where G is the shear modulus. The latter energy is of the second order in the effective pressure f/L. It is therefore much smaller than the Gibbs-Thomson term and may be typically ignored in the phase equilibrium conditions [14].

We are now prepared to consider evaporation of the cubic crystallite in Fig. 4. Detachment of a corner particle requires the same work $\mu_\infty \approx 3\varepsilon$ as detachment of the particle from the kink on an infinite crystal – because intermolecular interactions are of the short range nature, much shorter than the crystallite size. Therefore the detached particle "does not know" the size of the crystallite. (On the contrary, in a liquid droplet, the capillarity pressure and waves "lets each particle know" what the droplet size is). Detachment of a next particle from the crystallite along its upper right edge in the Fig 4 also requires the same work 3ε to be spent. Thus the Gibbs energy of crystallite-and-surrounding system does not change again since the chemical potential of the surrounding equals the potential of an infinite crystal. However, when the detachment process comes to the last particle in the edge row, only two bonds are needed to be ruptured for the detachment requiring the work of only 2ε. Here is where the crystallite size becomes effective. Disassembling the whole crystallite, one can easily come to the gain $\omega\alpha/L$ in the free energy as required by the GTL assuming $\alpha = \varepsilon/$ (surface area per contact between two particles). This disassembling procedure follows the Kaishev's method of the average detachment work (see, e.g. [14]). The simplified analysis here ignores vibration and other contributions to the chemical potential except for the intermolecular bonds, ε. The disassembling demonstrates, however, that the **GTL for crystals is valid only on average, while for liquids it is applicable for each detached particle**.

3. Applicability of GTL for spiral growth.

The BCF theory considers steps with **high kink density**. Such a step becomes a rounded spiral as it propagates around the immobile point D of a screw dislocation outcrop to the face. For the heavily kinked step to be immobile at D, it must acquire at that point the curvature of the circular 2D critical nucleus. Then, according to the GTL, the step is indeed at equilibrium with the surrounding solution at the point D. The rest of the step winds up to form a rounded steady state rotating spiral. The distance between the turns is proportional the nucleus size.

Similar situation holds, if the step is **less kinked** so that it is, on average, straight if parallel to the close packed orientations in the lattice (Sec.1). Nevertheless, the distance between kinks is assumed to be still essentially shorter that the edge lengths L_1, L_2 of the polygonal 2D critical nucleus. The latter is drawn in Fig. 5 as a rectangle near the dislocation outcrop D. In this case of the moderate kink density the first step segment adjacent to D is not supposed to propagate (crossed arrow in Fig.5) until it reaches the length L_2 (or L_1 for another orientation). This segment DA is elongating due to propagation of the next adjacent step segment (the arrow pointing left and down). As a result, the segment DA reaches the critical length L_2, starts to propagate and builds a new turn of the polygonal spiral. This is the well known process explained by the BCF theory. Subsequent stages of a polygonal spiral development on lysozyme crystal face are shown in Fig. 6. We shall see, however, that this spiral development suggests kinetic rather the thermodynamic approach described above.

Finally, let us consider a nearly **kink free** step segment. The kinks appear in pairs either by the "positive" 1D nucleation of a new molecular row at the step or by "negative" nucleation when a molecule or a piece of the last existing step row dissolves (Fig 3). The kink free state is possible if: 1. the kink nucleation rate (kink pairs/cm.s) is low; 2. the time when the step segment exists is short. The first segment adjacent to dislocation D develops because the next segment AA' propagates (Fig.7). Therefore a sufficiently short segment should be always kink free. That kink free segment is the longer the lower is the nucleation rate. In a supersaturated solution, only the positive nuclei are able to develop and, sooner or later, the positive nucleation prevails over local dissolution and the segment DA starts to propagate. The question is if the critical length when this propagation starts equals the edge of the 2D nuclei, i.e. if the GTL applies, or this critical length is other than the thermodynamic critical size (L_1 or L_2 in Fig.5).
We answer this question for the step with very low equilibrium kink density when $\exp(\varepsilon/kT) \ll 1$. Then in a supersaturated solution the local dissolution may be ignored. For the reasons discussed in Sec 2 the positive 1D nucleation rate (as well as the local dissolution rate) do not depend on the segment length and thus can not lead to the GTL unless another mechanism operates. The positive nucleation should move the DA segment forward at the rate depending only on this nucleation rate no matter what the GTL requires. Let the DA have moved to the position CB. The question is if CB will retreat if it is shorter than the critical size (L_2 in Fig. 5) - to decrease the system Gibbs free energy. This retreat is supposed to happen following the GTL if the relative supersaturation $S - 1 \equiv C/C_e = \Delta\mu_\infty/kT < \omega\alpha/kTL$. Here C and C_e are the actual and equilibrium solution concentrations, respectively.

The only mechanism that can implement the GTL is the kink exchange between the corners C and B. Namely, single species in the corners occupy the kink positions and may be detached splitting from the corners the kinks of the opposite signs and shifted towards the center of CB. After a first kink is formed at the sharp corner, the second, third, etc kink should appear – the corner becomes rounded. This rounding develops to increase the step entropy: each of the kinks split from the corner acquires the freedom to select its position between two neighbors (overlapping the intervals allowed for each kink is forbidden since high energy price of 2ε should be paid for resulting overhang). That

freedom means that there exists entropic repulsion between kinks. Random attachments and detachments of species to/from a kink at the frequencies w_+ and w_- force these kinks to diffuse along CB. Evidently, the kink diffusivity $D = a^2(w_+ + w_-)/2$. Diffusing along CB, the kinks of the opposite sign may meet one another and annihilate reducing the system energy by 2ε. Sequence of such annihilations assures the retreat of the segment CB, and decreases the system potential.

However, supersaturation hinders this annihilation. Indeed, the supersaturation $S>1$ means that the attachment frequency of the species at the kink, w_+ ,exceeds the detachment frequency w_-, so that the average kink rate $v = a(w_+ - w_-) > 0$. Therefore the kinks split from the corners are "pushed" against the entropic pressure, back to the corners. The balance is achieved when the kinks remain within the distance D/v near each corner. If the segment length L is shorter than $2D/v$ the kink exchange between the corners is efficient and the GTL is implemented. However, at $L >> 2D/v = a(w_+ + w_-)/(w_+ - w_-) = a(S+1)/2(S-1)$ the kinks generated by the opposite corners C and B may meet very rare so that annihilation is practically excluded and the GTL can not be implemented. Here we used the well known relationship $w_+/w_- = \exp(\Delta\mu/kT)$. Thus for the steps with low kink density the GTL may operate only for the segments $L < \sim 2a/(S-1)$. At $L/a = 100$, i.e. at $L< 50$nm for $a =5$Å, the GTL should operate only if supersaturation $S - 1 < 2a/L = 0.02 = 2\%$.

On the steps with a noticeable kink density, wandering kinks meet and annihilate at distances of the order of the average interkink distance rather the full segment length. In this case, communication between the corners and thus implementation of the GTL occurs via chain of consecutive kink meetings along the step segment. This is the case of intermediate kink density, Fig.5. For the same reason, there is no problem with the GTL on the rough steps and surfaces.

When the GTL is not effective, the typical length replacing the thermodynamic critical length $L_{1,2}$ is the kinetically determined average distance between kinks $\sim (v/J)^{1/2}$ where J is the positive kink nucleation rate.

Experimental facts on steps with low kink density are presented in [1,9,15-19]. In particular, the following facts suggest that the GTL may not operate:

1. On lysozyme, similar to other protein crystals, kinks may be directly visualized by atomic force microscopy (AFM) and may be directly counted (Fig 2). The critical segment length, L^*, above which the step segment adjacent to the screw dislocation or to the stacking fault outcrop start to propagate normal to itself may be also directly measured by AFM. The so found L^*'s turn out to be longer than or comparable to the interkink distance. Thus, indeed, there may be no kinks on the first step segment until it reaches the length sufficient for the kink generation.
2. On the (101) face of monoclinic lysozyme, the steps propagating in the opposite directions are parallel one another (Fig. 6) so that the 2D nucleus should be a rhombus. Therefore if the GTL operates the critical lengths L^* for the step segment looking in the opposite directions must be equal to one another. Experimentally, the L^*'s differ up to twice. This violation of symmetry is

explainable in kinetic terms: molecular structures of the step risers looking to the opposite directions are different. Different should be also the step free energies and kink generation rates. This is the generation rate that is supposed to control L^*. Indeed, according to the Wulf's theorem, the center from which the step energies plotted to find the equilibrium shape does not, generally speaking, coincide with the geometrical center of the resulting shape (the nucleus). The latter case it shown in Fig 5. The rhombic shape of the expected nucleus mentioned above forces the L^* for the steps looking in the opposite directions to be equally long, opposite to the experimental finding.

3. The measured L^* experience variations up to ±40% around its average while the experimental error is <15%. Such behavior is consistent with the kinetic process: the L^* is controlled by the length and time sufficient for kink generation, and should vary significantly since the kink nucleation is a random event and not too many kinks are needed to start the first segment propagation. As it was mentioned above, one should expect $L^* \sim (2v/J)^{1/2}$.
4. Assuming that the measured L^* still equals the edge of the 2D critical nucleus one may estimate the step riser free energy α. For monoclinic lysozyme, the so found α varies ~ 2-3 times, absolute value being from 4 to 30 erg/cm^2. For orthorhombic lysozyme, that estimate results in ~70erg/cm^2. The step riser energy following from the supersaturation dependence of the tetragonal lysozyme face growth rate by 2D nucleation is only ~ 1erg/cm^2, close to other proteins (in terms of ε). On calcite, the measured energy α well obeys linear dependence of the L^* on reciprocal supersaturation following from the BCF theory. However, the α turns out to be ~400erg/cm^2 vs ~100erg/cm^2 from nucleation data.

Difference in behavior between the steps with the high and low kink density stems from the well known concept that thermodynamic laws are implemented by trail and error events, i.e. by fluctuations. The steps with low kink density fluctuate slowly and thus require more time to implement the GTL. The longer the segment the more time is needed, the closer to equilibrium should be the system to obey thermodynamic rather than kinetic laws.

4. Small three dimensional crystallites.

As it was shown above, the GTL for a short step segment with low kink density is implemented via kink exchange between corners of the segment. Similarly, the GTL for a facetted 3 D crystallite should operate only via step exchange between edges limiting a face. This exchange starts with step splitting from the edges, i.e. with the rounding of the edges and apexes. The reason for splitting is entropic repulsion between steps: each step is allowed to meander only between its two neighbors. Radius of the corner rounding decreases as the ε/kT ratio and supersaturation increases.

Let us assume that the edge and apex rounding spreads over a small portion of the cubic crystallite face and that the crystallite is larger than the 3D critical nucleus for the given supersaturation $\Delta\mu$, $L > 4\omega\alpha/\Delta\mu$ (Fig. 8a,b). In absence of dislocations, the facet propagation rate is controlled by 2D nucleation. The edge of the square-shape 2D

nucleus or of the outer diameter of the disc-shape nucleus equals $2\omega\alpha/\Delta\mu$, twice less the facet size of the 3D nucleus. Thus there are steps loops supercritical with respect to the 2D nucleation but smaller than the facet size: $2\omega\alpha/\Delta\mu < 2l < L$ (Fig.8). The 2D nucleation rate J_2 (nuclei/cm^2.s) is the same as on the infinite crystal face since the species, their sub- or supercritical clusters do not "know" the crystallite size, i.e. the J_2 is independent of L. The lower effective J_2 may be tuned to the GTL by fluctuations only, i.e. by elimination of the excess crystalline layer(s) as soon as they appear. For instance, let the upper layer shown in Fig 8a as a circular disk should collapse. If that removal happens, the effective nucleation rate will be lower than that of the infinite face thus implementing the GTL. This process is similar to retreat of the protruded segment CB in Fig. 7.

Shrinking of an island by a single particle detachment diminishes the free energy of the system only if the disc diameter $2l < 2\omega\alpha/\Delta\mu$, the diameter of a critical nucleus ($2l$ is on the left from the maximum on the lower curve in Fig. 8b showing dependence of the Gibbs free energy on the 2D cluster size). Otherwise, for the shrinking, the system must overcome the potential barrier by fluctuations. The barrier is the higher the more the island size $2l$ exceeds the critical size $2\omega\alpha/\Delta\mu$. In other words, as soon as the new island reaches the supercritical size, i.e. $2l > 2\omega\alpha/\Delta\mu$, the island has two options: 1. to proceed growing with the growth driven by systematic decrease of the system potential or 2.

to shrink back to a subcritical size over the potential barrier. Clearly, the first option has higher chance to be taken. These arguments suggest that the considered crystallite should grow at the 2D nucleation rate ignoring the GTL. Of course, the overall facet normal growth rate is $\sim L^2$ until the crystallite size $L < (v_{st}/J_2)^{1/3}$ where v_{st} is the step rate [14].

The situation is different if the edge and apex rounding is spread over the crystallite face leaving a flat terrace of the size $\sim 2\omega\alpha/\Delta\mu$ or less near the face center even in the supersaturated solution (that should happen close to the roughening transition). Then the top layer easily collapses and the effective 2D nucleation rate will be tuned to implement the GTL. The GTL should also be effective if a screw dislocation leads the growth of the crystallite face or point defects decrease the potential barrier for the top layer collapse. Evidently, the GTL is always valid for the crystallites with rough surfaces.

We are not aware of experiments with 3D crystallites that may confirm or disprove these predictions. It is well known however that a small crystallite in a vapor seen at equilibrium as a sphere only slightly truncated by the close packed facets becomes a polygon in a supersaturated vapor – the growth rate anisotropy is much stronger than that of the free surface energy.

5. Conclusions

Thermal fluctuations are insufficiently fast to ensure high kink density on steps on a crystal interface if kink energy noticeably exceeds kT, i.e. the transformation enthalpy is large. Proteins and slightly soluble salts serve as examples.

For short step segments with low kink density and for small well facetted 3D crystallites the Gibbs-Thomson correction to the crystallization driving force is valid only very close to equilibrium.

6. **Acknowledgements**

This work was performed partly under the auspices of the US Department of Energy by the University of California, Lawrence Livermore National Laboratory under Contract No. W-7405-Eng-48. Support from the Basic Energy Sciences office of the Department of Energy, NASA grant NAG8-1927 and Russian Foundation for Fundamental Research under the grant 03-02-1611 is also deeply acknowledged.

References

1. A.A.Chernov, J.J.DeYoreo, L.N.Rashkovich, P.G.Vekilov MRS Bulletin, 29(2004)927-934
2. 2. W.K.Burton, N.Cabrera, F.C.Frank, Phil Trans. Roy.Soc. London Ser A243(1951)249-358
3. V.V.Voronkov, Sov Phys Crystallography, 15(1970)8;
4. V.V.Voronkov, Sov Phys Crystallography, 18(1972)19-23;
5. V.V.Voronkov in Crystals.Growth.Properties.Applications. Springer, Berlin 9(1983)75-111
6. S.-T.Yao, D.N.Petzev, B.R.Thomas, P.G.Vekilov, J.Mol.Biol. 303(2000)667
7. A.E.Nielsen J.Crystal Growth 67(1984)289-310;
8. J.Cristoffersen, E.Rostrup, M.R.Cristoffersen, J.Crystal Growth 113(1991)599-605
9. L.E.Wasylenki, P.M.Dove, D.S.Wilson, J.J.De Yoreo, Geochim. Cosmochimica Acta 69(2005)3017
10. G.W.Gibbs, Scientific Papers, I (Dover, N.Y. 1957)
11. J.W.Cahn, Acta Metall. 28(1980)1333
12. W.W.Mullins, J.Chem. Phys. 81(1984)1436
13. M.C.Payne, N.Roberts, R.J.Needs, M.Needs, J.D.Johannopulos, Surface Sci. 211/212(1989)1
14. A.A.Chernov Modern Crystallography III. Crystal growth. Springer Ser Solid State, vol 36, Springer Berlin Heidelberg, 1984
15. K.J.Davis, P.M.Dove, J.J.De Yoreo, Science 290(2000)1134
16. H.H.Teng, P.M.Dove, C.A.Orme, J.J.De Yoreo, Science 282(1998)724
17. L.N.Rashkovich, E.V. Petrova, O.A.Shustin, T.G.Chernevich, Phys Sol State 45(2003)377
18. L.N.Rashkovich, N.V.Gvozdev, M.I.Sil'nikova, A.A.Chernov, Kristallografiya 47(2002)923

19. A.A.Chernov, L.N.Rashkovich, I.V.Yaminski, N.V.Gvozdev, J.Phys: Condens. Matter 11(1999)9969
20. A.A.Chernov, L.N.Rashkovich, P.G.Vekilov, J.Cryst.Growth 275(2005)1

Figure Captions

Fig.1. Steps with high kink density on the (111) face of a ferritin crystal. AFM image. Steps are marked by numbers nearby. Each ferritin molecule is a sphere 13nm in diameter seen on the terraces between steps. The panel below shows probability distribution of interkink distances at relative supersaturation $\sigma = \Delta\mu/kT = 1.1$ [6].

Fig.2. Single kink on a the step on orthorhombic (left) and rare kinks on the steps on the monoclinic (right) lysozyme faces. In the former, molecular rows are visible on the terraces on the both sides of the step seen as the bold dark line. On the left, the step is one lattice spacing (7.37nm) high, the kink is one lattice spacing (5.65nm) deep. Average kink density on the monoclinic lysozyme is 2.10^{-3} 1/nm (interkink distance is 490nm), lattice spacing along the steps is 6.5nm. Each view field is 3.5x7μm.

Fig 3. Horizontal and vertical steps (in bold) cross one another and create reentrant corner on the left. Three kinks of the same sign are split from the corner and are supposed to move to the right. Each rectangle with a backslash symbolizes a molecule. Two molecules may be considered as a stable "positive" 1-Dimensional (1D) nucleus if this molecular pair does not decay loosing one or all two of these molecules due to thermal fluctuations. The dip on the right between two kinks of the opposite signs may appear via detachment of a molecule (a "negative" 1D nucleus) from a kink free straight step portion and subsequent detachment of molecules occupying the so opened two kink positions. In a supersaturated solution, the dip is ultimately filled and disappears so that only positive nuclei are stable. The negative nuclei are stable in the undersaturated solution. An impurity particle (shaded) adsorbed at the step may also initiate a "positive"1D nucleus.

Fig 4. The Gibbs-Thomson law (GTL) is implemented differently in liquids (left) and in solids (right). In liquids, the work required to detach each and ever molecule from a liquid droplet, i.e. the chemical potential, does depend on the actual droplet size (see the text). In crystals, the detachment work depends on the crystallite size only on the average over either the whole crystal or the crystalline layer or the row. To illustrate this averaging, the molecular row shown on the right upper face of the cubic crystal is supposed to be dissolved molecule by molecule in the direction indicated by the arrow. To detach all but the last particle from the crystal one needs to spend the same work 3ε as that from a kink on an infinite crystal surface. However, detachment of the last particle

in the row requires 2ε. Thus, averaging over the row results in the GT decrease of the chemical potential by the energy inversely proportional to the row length. Thus the chemical potential of the species in the regular kink position does not depend on the crystal size - when interactions between molecules span over the range much shorter than the crystallite size.

Fig. 5. The polygonal spiral consisting of straight step segments around the outcrop D of the screw dislocation to the face. The segments are supposed to contain kinks the distance between which is shorter than the segment length. The first segment, DA, do not propagate (crossed arrow) until it reaches the length of the cristallographically identical edge of the critical nucleus shown in the middle.

Fig. 6. Subsequent stages of polygonal spiral development on monoclinic lysozyme.

Fig. 7. Same as the Fig. 5 but for the about kink free step. The segment DA is supposed to shift to the position CB via several acts of 1D kink nucleation and stays kink free. If DA is shorter than the edge of the 2D critical nucleus the GTL requires DA to retreat. The mechanism is based on the kink exchange between the apexes C and B. Namely, the kinks of the opposite sign split from C and B due to random thermal detachment of species. However, in a supersaturated solution, these kinks are pushed back since attachment frequency exceeds the detachment frequency. As a result, on average, the kinks are unable to depart from B and C further than by the distance D/v and annihilate if the segment length $L >> D/v$. Thus the GTL operates only if $L < D/v$.

Fig.8. Implementation of the Gibbs-Thomson law on a small facetted crystallite in a supersaturated solution. The crystallite grows by 2D nucleation on its faces, with the nucleation rate independent of the face size (Sec. 2). Therefore, to implement the GTL, the surface layers should dissolve if the crystallite is smaller that the 3D critical nucleus $4\omega\alpha/\Delta\mu$ for the given supersaturation$\Delta\mu$. (a): A circular step loop split from the face edge due to entropic repulsion from the edge. If the loop is supercritical, i.e. its diameter $2l$ exceeds the diameter $2\omega\alpha/\Delta\mu$ of the 2D critical nucleus the loop can not dissolve unless it overcomes a part of the 2D potential barrier shown in the lower curve in (b). The upper curve in (b) shows, for comparison, the Gibbs free energy of the system for creation of the 3D cubic crystallite of the size L.

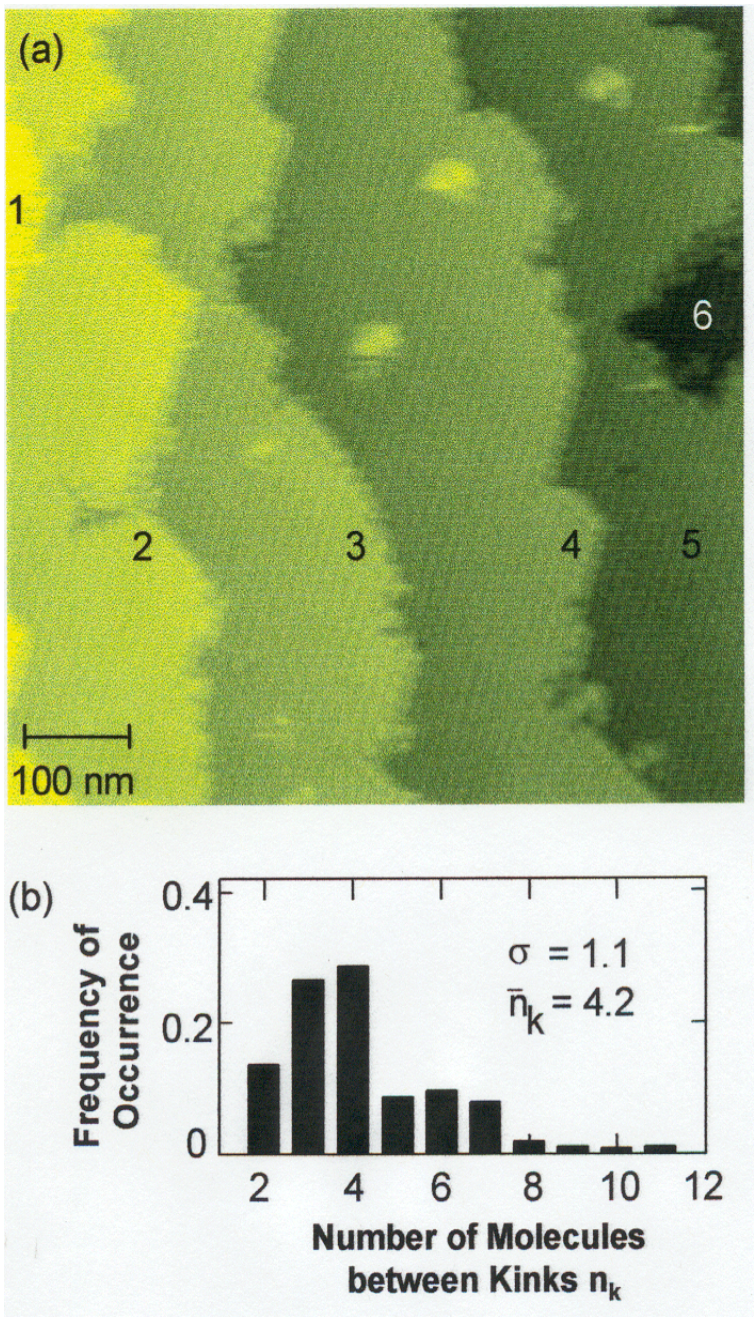
(a)
1
2
3
4
5
6
100 nm
(b)
Frequency of Occurrence
0.4
0.2
0
σ = 1.1
$\bar{n}_k$ = 4.2
2
4
6
8
10
12
Number of Molecules between Kinks n_k

Fig 1

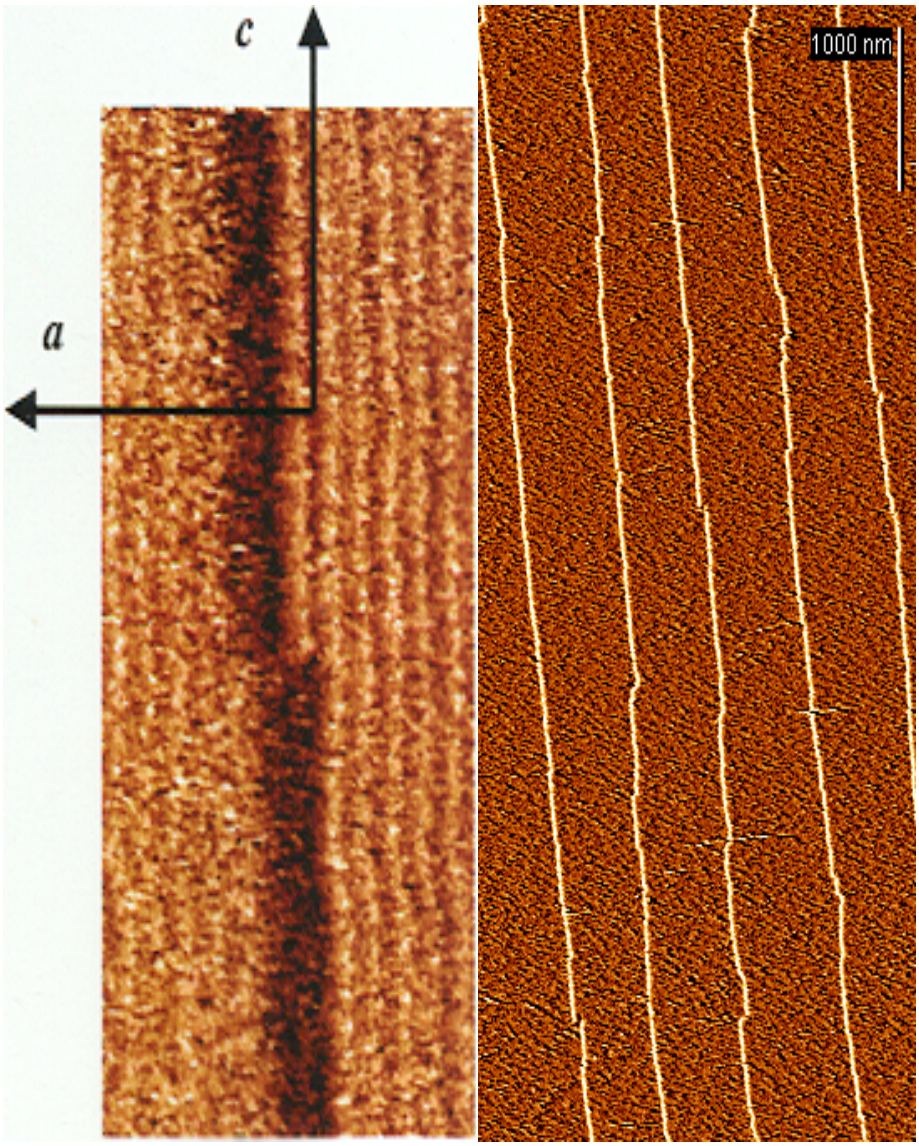

Fig. 2

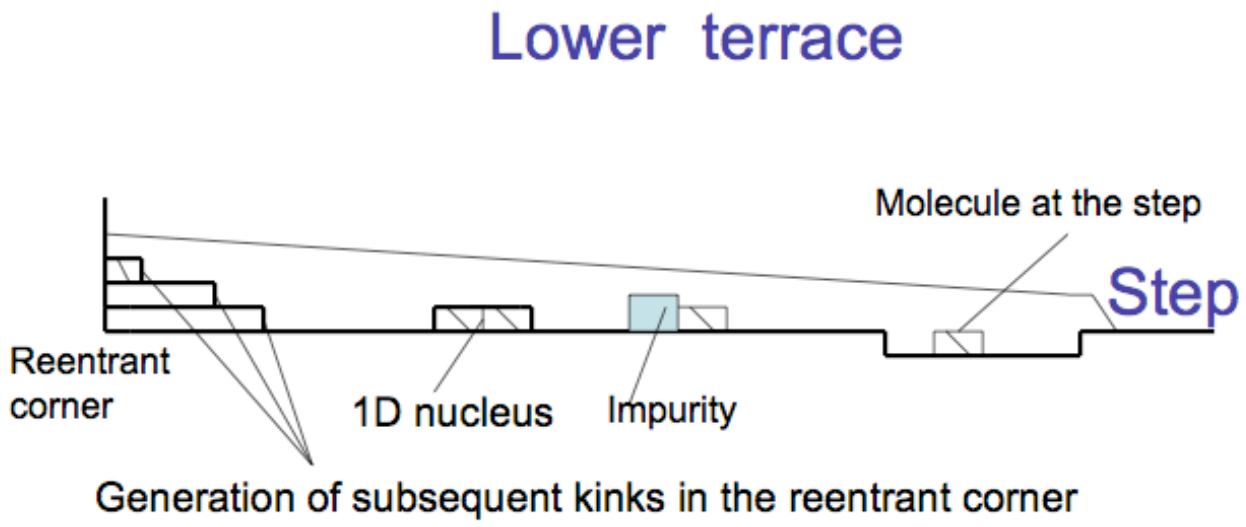
Lower terrace
Molecule at the step
Step
Reentrant corner
1D nucleus
Impurity
Generation of subsequent kinks in the reentrant corner
Upper terrace

Fig 3

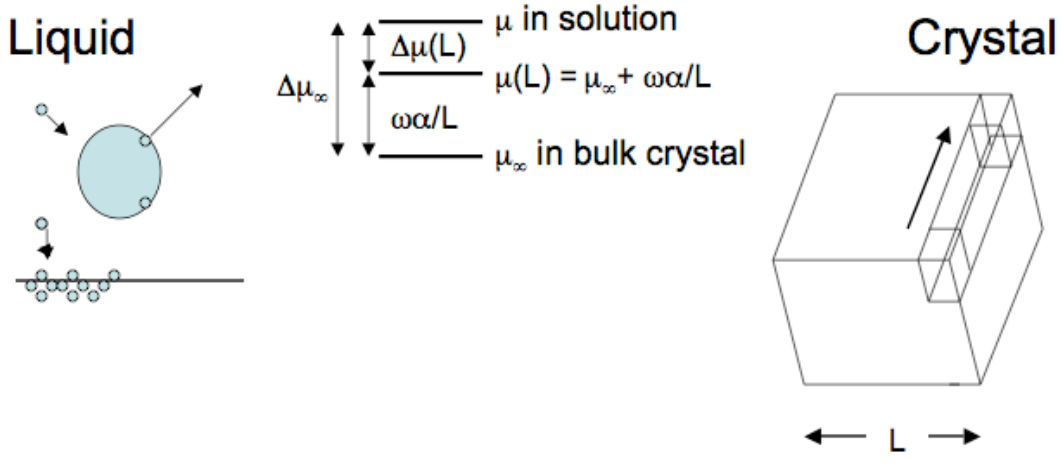
Liquid
Δμ∞
Δμ(L)
ωα/L
μ in solution
μ(L) = μ∞+ ωα/L
μ∞ in bulk crystal
Crystal
L

Fig 4

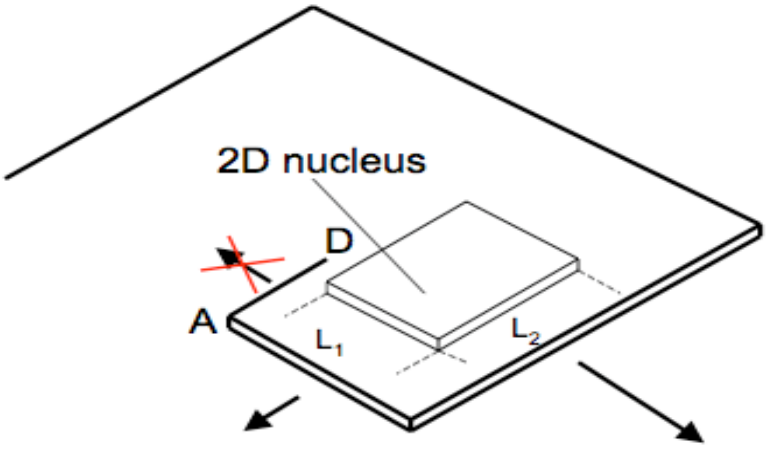

Fig 5

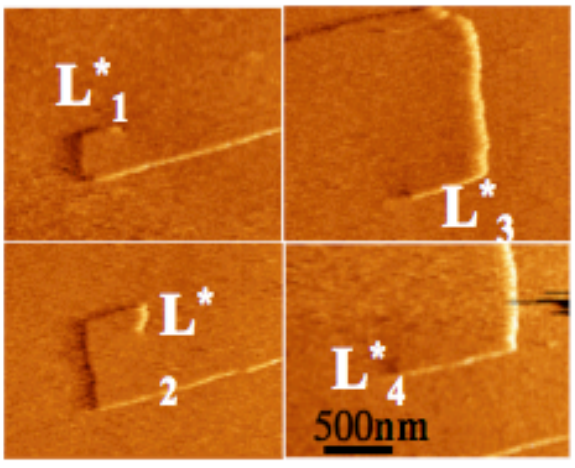

Fig 6

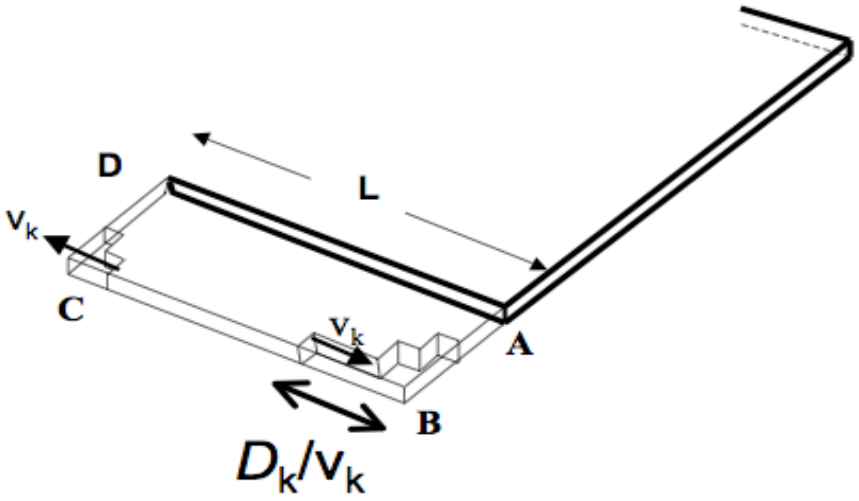

Fig 7

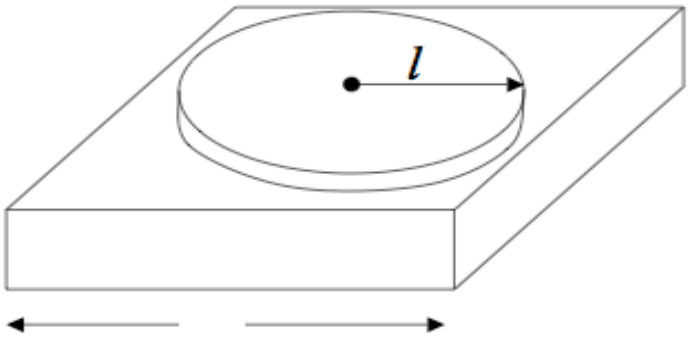

Fig 8a

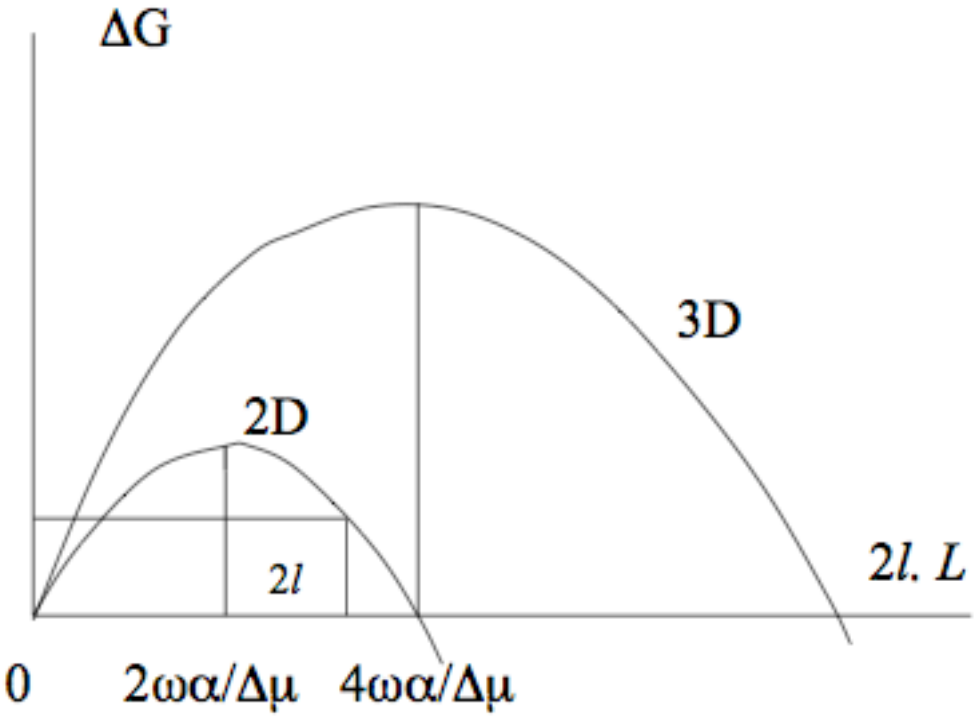

Fig. 8b